In Situ Estimates of Sub-Crustal Continental Lithospheric Heat Flow: Application to the Slave and Kaapvaal Cratons

Paul Morgan[1,2] and **Suzanne Y. O'Reilly**[2]

[1] *Department of Geology, Box 4099, Northern Arizona University, Flagstaff, AZ 86011-4099, USA.*

[2] *ARC National Key Center for Geochemistry and Metallogeny of Continents (GEMOC), Department of Earth and Planetary Sciences, Macquarie University, NSW 2109, Australia.*

Basic Physics of Lithospheric Heat Flow

Once a section of lithosphere is formed, continental or oceanic, and is no longer actively deforming, its interactions with the underlying mantle are mostly limited to a small flow of heat into the base of the lithosphere, controlled by the thermal gradient in the lowermost lithosphere, perhaps accompanied by small-scale convection. These conditions may change significantly if a rising mantle plume, 200°C or much hotter than undisturbed temperatures, impinges upon the base of the lithosphere, resulting in the injection of heat through magma and other fluids into the lithosphere. Magma commonly reaches the surface as volcanism during these events, but unless a large volume of magma is intruded into the lithosphere, or a large volume of hot material remains in the sub-lithospheric plume head, there will not be a significant transient perturbation of lithospheric temperatures.

The thermal relaxation time of oceanic lithosphere, the time taken for hot lithosphere to cool to thermal equilibrium with the convecting sub-lithospheric asthenosphere is constrained to 70-100 Ma (Stein and Stein, 1992), the age range at which most ocean floor flattens and appears to stop cooling and thermally contracting. This relaxation time corresponds to a lithospheric thickness of 100-125 km, consistent with the seismic and elastic thickness estimates of lithospheric thickness in the ocean basins.

Continental lithosphere, unlike oceanic lithosphere, is heterogeneous, and relaxation times are generally longer and have a greater range. They have a greater range because stable continental lithosphere varies in thickness, probably from <100 km to >250 km. Relaxation times are generally longer for two reasons: 1) in general, stable continental lithosphere is thicker than oceanic lithosphere; and 2) erosion or sedimentation may prolong the relaxation process (Morgan, 1984; Morgan and Sass, 1984). However, even with these complicating factors, the global data set indicates that thermal relaxation of continental lithosphere is complete by about 250 Ma. Hence, regions with tectonothermal ages (ages of the last major tectonic and/or magmatic event) of Paleozoic and older, may be assumed to have lithosphere in steady-state thermal equilibrium. Temperature is a fundamental parameter in controlling physical properties within the lithosphere. Unraveling lithospheric thermal structure, the geotherm, is therefore of first order importance.

Continental Heat Flow

Although in terms of thermal relaxation, the basic physics that describes the cooling of continental and oceanic lithosphere is similar, the global heat flow data set shows that surface heat flow from continental sites with tectonothermal ages of Paleozoic and older show considerable scatter (Figure 1), much greater than the scatter measured in ocean basin heat flow. The large scatter in heat flow values from stable continental regions is not an artifact of measurement errors or local site conditions as can be seen from the significantly lower standard deviation for data from Archean tectonothermal age than for data from Proterozoic and Paleozoic sites. The dominant contribution to the lateral variability in surface heat flow in stable continental lithosphere is the heterogeneous distribution of radiogenic heat production in continental lithosphere, primarily, the variability of concentrations of the unstable isotopes ^{232}Th, ^{238}U, ^{40}K, and ^{235}U in the upper crust.

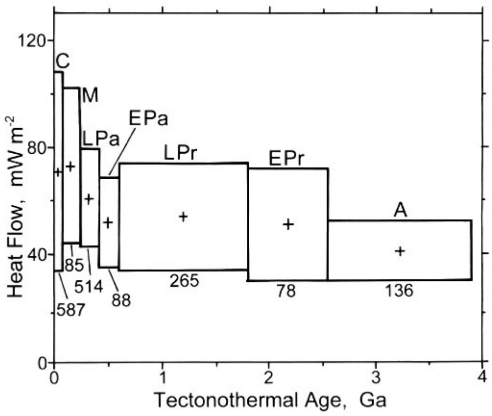

Figure 1. Average continental heat flow versus tectonothermal age in billions of years (Ga), the age of the last major tectonic or magmatic event at the heat flow site. Data are grouped in geological age ranges: C-Cenozoic; M-Mesozoic; L Pa-Late Paleozoic; E Pa-Early Paleozoic; L Pr-Late Proterozoic; E Pr-Early Proterozoic; A-Archean. Crosses are plotted at the mean heat flow and the midpoint of the age range and box heights indicate $\pm$ one standard deviation of the heat flow data about the mean. Numbers below the boxes indicate the number of data in each group. From Morgan (1984).

In relatively homogeneous crustal terrains the upper crustal radiogenic component of heat flow can be separated from the deeper heat flow component if certain conditions are met. This analysis yields a depth scaling parameter, *b*, for the distribution of upper crustal radiogenic heat production, and the deeper component of heat flow, know as the *reduced heat flow* (Morgan, 1984). Using this analysis for heat flow provinces of different tectonothermal ages indicates that the reduced heat flow does not significantly change for provinces of Late Paleozoic age and older, but that Archean crust has, on average, significantly less U, Th, and K than younger crust (Morgan, 1985), a result consistent with chemical studies (Taylor and McLennan, 1981, 1983)

Extrapolated Continental Lithospheric Geotherms

Lithospheric temperatures may be extrapolated from the surface to depth assuming steady-state conductive conditions. Examples of such geotherms are given in Figure 2. An exponential decrease in radiogenic heat production from the surface, with b as the exponential decrement, is used as this distribution allows the relation to survive differential weathering (Lachenbruch, 1968). As can be seen from these model geotherms, all calculated with the same heat input below the upper crustal zone of heterogeneous radiogenic heat production enrichment, *i.e.*, the same reduced heat flow, a wide range of lithospheric mantle temperatures and corresponding lithospheric thicknesses are predicted. Greater uncertainties are introduced when uncertainties in lower crustal and uppermost mantle radiogenic heat productions and thermal conductivities are introduced into the models.

Figure 2. Model Geotherms for stable continental lithosphere with the same reduced heat flow and a range in crustal heat production. The geothermal correspond to a reduced heat flow of 27 mW m^{-2}, a crustal thermal conductivity of 2.5 W m^{-1} K^{-1}, and a temperature dependent mantle thermal conductivity (see below). A uniform heat production of 0.05 µW m^{-3} was assumed for the mantle, with a crustal thickness of 35 km. The horizontal dashed line labeled Moho shows the crust/mantle boundary. The solid line labeled **BDS** is an approximation to the basalt dry solidus and gives one interpretation of the maximum possible temperature/thickness of the lithosphere. Solid curves labeled 1, 2, and 3 correspond to geotherms calculated for a b of 10 km with an exponential decrease starting at 0, 2, and 6 µW m^{-3}, respectively. Dashed curves labeled 4 and 5 correspond to geotherms calculated for a b of 15 km with an exponential decrease starting at 2 and 6 µW m^{-3}, respectively.

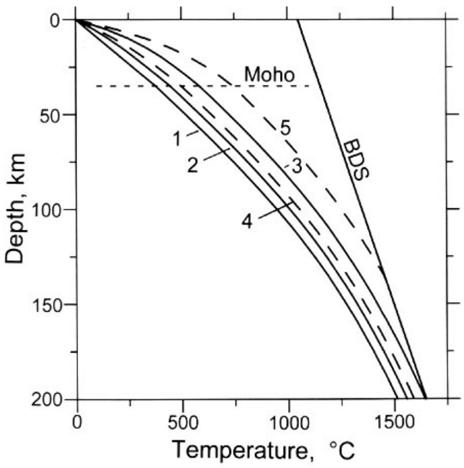

Mantle Lithosphere Thermal Conductivity

In order to use temperature and depth (pressure) data calculated from geothermometry and geobarometry studies of mantle xenoliths to calculate mantle lithosphere heat flow, we have started a program of high temperature thermal conductivity measurements of mantle xenoliths. Preliminary results from these studies are summarized in Figure 3. From these studies we have established a preliminary temperature-dependant 3rd-order approximation for the thermal conductivity of the mantle lithosphere, K_{ml} as follows:

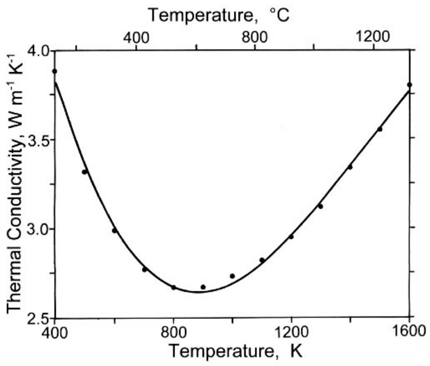

Figure 3. Model thermal conductivity of mantle lithosphere as a function of temperature. Direct determinations of thermal conductivity to 900°C of lherzolite xenolith samples 30 mm x 30 mm x 10 mm thick in a modified steady-state divided-bar apparatus have yielded thermal conductivities within error limits of the single-crystal olivine results of Schatz and Simmons (1972; Morgan and O'Reilly, 2001). Olivine has a minimum conductivity at ~600°C, above which temperature radiative thermal conductivity becomes significant. Dots on graph show smoothed results. Curve is 3rd-order polynomial fit to data.

$$K_{ml} = 7.40 - 1.27\text{x}10^{-2}\, T_K + 1.04\text{x}10^{-5}\, T_K^2 - 2.43\text{x}10^{-9}\, T_K^3 \qquad (1)$$

where T_K is the absolute temperature.

Slave Craton Mantle Lithosphere Heat Flow

Temperature and depth estimates for xenolith samples from the Slave Craton beneath the Lac de Gras region (Griffin et al., 1999) are plotted in Figure 5. A crude estimate of the mantle lithosphere geotherm has been calculated from these data using a linear least-squares fit to the data, the result of which is plotted on the figure, and which yields an average geothermal gradient of 6.2 ± 3.9 (± 1 s.d.) °C km^{-1}. The thermal conductivity over the depth range covered by these data was calculated by using the regression curve to estimate maximum and minimum temperatures applicable to the depth range of the xenoliths, then using equation 1 to compute conductivity values at intervals of 1°C over this temperature range and calculating a harmonic mean conductivity (the harmonic mean is more applicable to heat flow calculations than the arithmetic mean). The calculated harmonic mean thermal conductivity was 3.1 $\pm$ 0.2 W m^{-1} K^{-1}. Conductive heat flow is the product of geothermal gradient and conductivity of the rocks over which the gradient is measured, yielding an estimated mantle lithosphere heat flow for the Slave Craton of 19.0 $\pm$ 12.0 mW m^{-2}.

Figure 4. Plot of temperature vs. depth (pressure) estimated for xenoliths from the Slave Craton based on geothermometry and geobarometry data. The solid line shows a linear least-squares fit to the data with a gradient of 6.2 $\pm$ 3.9 ($\pm$ s.d.) °C km^{-1}.

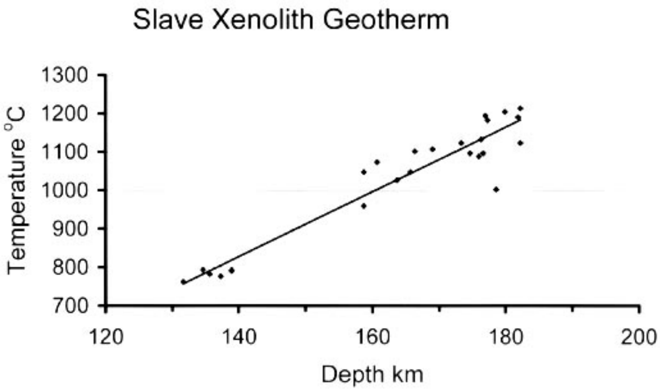

Kaapvaal Craton Mantle Lithosphere Heat Flow

Similar data have been studied using analyses of xenoliths from the Kaapvaal craton from a range of different localities across the craton including a concentration near the southern margin (Pearson et al., 1995), and temperature and depth data from these studies are plotted in Figure 5. Geothermal gradient, harmonic mean thermal conductivity, and heat flow values were determined as for the Slave Craton using the Kaapvaal xenolith data with the following results: lithospheric mantle geothermal gradient = 4.6 $\pm$ 2.2 °C km^{-1}; harmonic mean thermal conductivity applicable to gradient interval = 2.9 $\pm$ 0.1 W m^{-1} K^{-1}; Kaapvaal lithospheric mantle heat flow = 13.5 $\pm$ 6.5 mW m^{-2} (all errors $\pm$ 1 s.d.).

Discussion

P-T and geotherm data have been previously published for xenoliths from both the Slave and Kaapvaal Cratons, but the data presented here represent a consistent treatment of samples and data manipulation. The values of mantle lithosphere heat flow estimated for the Slave and Kaapvaal Cratons are not significantly different within one standard deviation error limits, but both clearly indicate that reduced heat flow from surface heat flow vs. heat production plots is not equivalent to mantle heat flow. Approximately 10-15 mW m^{-2} of the reduced heat flow component must come from sources not recognized in the upper crustal radiogenic enriched zone of from mantle heat flow.

A mantle heat flow estimate for the eastern Canadian Shield extrapolated by Mareschal et al. (2000) from surface heat flow data by making various assumptions about the distribution of radiogenic heat production with depth is similar to the value estimated here for the Slave Craton. Jones (1988) extrapolated a slightly higher mantle heat flow value for the

Kaapvaal Craton than estimated here, although still within the 1 s.d. error limits. Surface heat flow is slightly higher in the Slave Craton (50 mW m^{-2}; Lewis and Wang, 1992) than sub-sediment heat flow in the Archean portions of the Kaapvaal Craton (~43.5 mW m^{-2}; Jones, 1988). This is most likely due to higher heat production in the upper crust of the Slave Craton than in the Kaapvaal Craton, which would result in an offset in the geotherm as shown in Figure 2. Such an offset is not visible in the xenolith P-T data (Figures 4 and 5), however, indicating that the effect is lost in the experimental scatter in the data. We hope that additional xenolith data will allow the refinement of mantle lithosphere Geotherms and heat flow estimates to allow the study of the effects of changes in upper crustal heat production on the geotherm (Figure 2) and to determine if variations in cratonic lithospheric heat flow are significant.

References Cited

Griffin, W.L., Doyle, B.J., Ryan, C.G., Pearson, N.J., O'Reilly, S.Y., Davies, R., Kivi, K and van Achterberg, E., 1999, Layered Mantle Lithosphere in the Lac de Gras Area, Slave Craton: Composition, Structure and Origin, *J. Petrology*, *40*, 705-727.

Jones, M. Q. W., 1988, Heat flow in the Witwatersrand basin and environs and its significance for the South African Shield geotherm and lithospheric thickness, *J. Geophys. Res., 93*, 3243-3260.

Lachenbruch, A. H., 1968, Preliminary geothermal model of the Sierra Nevada, *J. Geophys. Res, 73*, 6977-6989.

Lewis, T. J., and Wang, K., 1992, Influence of terrain on bedrock temperatures, *Global and Planetary Change, 98*, 87-100.

Mareschal, J. C., Jaupart, C., Gariépy, C., Cheng, L. Z., Guillou-Frottier, L., Bienfait, G., and Lapointe, R., 2000, Heat flow and deep thermal structure near the edge of the Canadian Shield, *Can. J. Earth. Sci., 37*, 399-414.

Morgan, P., 1984, The thermal structure and thermal evolution of the continental lithosphere, *Phys. Chem. Earth, 15,* 107-193.

Morgan, P., 1985, Crustal radiogenic heat production and the selective survival of ancient continental crust*, J. Geophys. Res., 90, Supplement*, C561-C570.

Morgan, P., and O'Reilly, S. Y., 2001, *In situ* estimates of sub-continental lithospheric heat flow from measurements on mantle xenolith samples, manuscript in preparation.

Morgan, P., and Sass, J. H., 1984, Thermal regime of the continental lithosphere*, J. Geodynamics, 1*, 143-166.

Pearson, N.J., O'Reilly, S.Y. and Griffin, W.L., 1995, The crust-mantle boundary beneath cratons and craton margins: a transect across the southwest margin of the Kaapvaal craton, *Lithos*, *36*, 257-288.

Schatz, J., and Simmons, G., 1972, Thermal conductivity of earth materials at high temperatures, *J. Geophys. Res., 77*, 6966-6983.

Stein, C. A., and Stein, S., 1992, A model for the global variation in oceanic depth and heat flow with lithospheric age, *Nature, 359*, 123-129.

Taylor, S. R., and McLennan, S. M., 1981, The composition and evolution of the continental crust: rare earth element evidence from sedimentary rocks, *Phil Trans. R. Soc. Lond., A, 301*, 381-399.

Taylor, S. R., and McLennan, S. M., 1983, Geochemistry of Early Proterozoic sedimentary rocks and the Archean/Proterozoic boundary, in Medaris, L. G., Jr., Byers, C. W., Mickelson, D. M., and Shanks, W. C., *Proterozoic Geology, Selected Papers from an International Symposium, Geol. Soc. Am., Memoir 161*, Boulder, Colorado, pp. 119-131.